Activation of the GPX4/TLR4 Signaling Pathway Participates in the Alleviation of Selenium Yeast on Deltamethrin-Provoked Cerebrum Injury in Quails

Jiayi Li[1] · Zhongxian Yu[2] · Bing Han[1] · Siyu Li[1] · Yueying Lv[1] · Xiaoqiao Wang[1] · Qingyue Yang[1] · Pengfei Wu[1] · Yuge Liao[1] · Bing Qu[1] · Zhigang Zhang[1,3]

Abstract

Deltamethrin (DLM) is a member of pyrethroid pesticide widely applied for agriculture and aquaculture, and its residue in the environment seriously threatens the bio-safety. The cerebrum might be vulnerable to pesticide-triggered oxidative stress. However, there is no specific antidote for treating DLM-triggered cerebral injury. Selenium (Se) is an essential trace element functionally forming selenoprotein glutathione peroxidase (GPX) in antioxidant defense. Se yeast (SY) is a common and effective organic form of Se supplement with high selenomethionine content. Accordingly, this study focused on investigating the therapeutic potential of SY on DLM-induced cerebral injury in quails after chronically exposing to DLM and exploring the underlying mechanisms. Quails were treated with/without SY (0.4 mg kg^{-1} SY added in standard diet) in the presence/absence of DLM (45 mg kg^{-1} body weight intragastrically) for 12 weeks. The results showed SY supplementation ameliorated DLM-induced cerebral toxicity. Concretely, SY elevated the content of Se and increased GPX4 level in DLM-treated quail cerebrum. Furthermore, SY enhanced antioxidant defense system by upregulating nuclear factor-erythroid-2-related factor 2 (Nrf2) associated members. Inversely, SY diminished the changes of apoptosis- and inflammation-associated proteins and genes including toll-like receptor 4 (TLR4). Collectively, our results suggest that dietary SY protects against DLM-induced cerebral toxicity in quails via positively regulating the GPX4/TLR4 signaling pathway. GPX4 may be a potential therapeutic target for insecticide-induced biotoxicity.

Keywords Deltamethrin · Cerebrum injury · Selenium yeast · Oxidative stress · GPX4/TLR4 · Apoptosis

Abbreviations

DLM	Deltamethrin
Se	Selenium
GPX	Glutathione peroxidase
GSH	Glutathione
ROS	Reactive oxygen species
GSSG	Disulfide glutathione
SY	Selenium yeast
SOD	Superoxide dismutase
MDA	Malondialdehyde
TLR4	Toll-like receptor 4
NF-κB	Nuclear factor-kappa B
Nrf2	Nuclear factor-erythroid-2-related factor 2
TNF-α	Tumor necrosis factor-alpha
GAPDH	Glyceraldehyde-3-phosphate dehydrogenase
WBC	White blood cell
RBC	Red blood cell
ICP-MS	Inductively coupled plasma mass spectrometry
H&E	Hematoxylin and eosin
TUNEL	Terminal deoxynucleotidyl transferase-mediated dUTP nick-end labeling
TBST	Tris-buffered saline and 20% Tween 20
PPI	Protein–protein interaction
SEM	Standard error of mean
NQO1	Nicotinamide adenine dinucleotide phosphatase: quinone acceptor 1
HO-1	Heme oxygenase-1

✉ Zhigang Zhang
zhangzhigang@neau.edu.cn

1 College of Veterinary Medicine, Northeast Agricultural University, 600 Changjiang Road, Harbin 150030, China

2 Pharmacy Department, The Affiliated Hospital To Changchun University of Chinese Medicine, 1478 Gongnong Road, Hongqi Street, Chaoyang District, Changchun, Jilin Province 130021, China

3 Heilongjiang Key Laboratory for Laboratory Animals and Comparative Medicine, Harbin 150030, China

iNOS   Inducible nitric oxide synthase
COX-2   Cyclooxygenase-2
JNK3   Jun N-terminal kinas e3
Bax   B cell lymphoma gene 2-associated X protein
Keap1   Kelch-like ECH-associated protein 1

Introduction

Pyrethroids, as a new generation of compounds in recent years, have gradually replaced traditional insecticides, which is inseparable from its low persistence, easy metabolism, high efficacy, and low toxicity to mammals and birds [1, 2]. Deltamethrin ([(S)-cyano-(3-phenoxyphenyl)methyl] (1R,3R)-3-(2,2-dibromoethenyl)-2,2-dimethylcyclopropane-1-carboxylate, DLM), an α-cyano type-II synthetic pyrethroid, is one of the most important pyrethroids first marketed in 1977 [2, 3]. DLM has been widely used within the agriculture and aquaculture based on its ability to effectively control and prevent pests such as mites, aphids, sea lice, grubs, beetles, and weevils [4–6]. Although DLM was initially thought to be less toxic, studies have demonstrated the toxicity of DLM on nontarget organisms, such as earthworm, lobster, zebrafish, and even humans [3, 7–9]. This is closely related to the residues of DLM to soil and water sources in the process of widespread use. Exposure to DLM may cause the damage of multiple tissue and organ toxicity, such as cardiac, neuro, hepatopancreas, cardiovascular, and testicular, and induce varying degrees of histopathological changes [10–13]. Hence, clarifying the key mechanism of DLM-induced potential injury may lead to beneficial therapeutic targets for DLM poisoning.

One of the main pathophysiological mechanisms by which DLM mediates organ injury is oxidative stress [14]. Studies have confirmed DLM-induced oxidative damage and biochemical alterations in organs and cells including hepatopancreas, embryos, and oocytes [15–18]. The cerebrum is an organ with high oxygen consumption and rich lipid, which might be vulnerable to oxidative stress caused by pesticides [19]. For instance, glutamate changed oxidative stress indices in adult albino rat cerebrum, leading potential oxidative damage [20]. Accordingly, we speculate that DLM may cause a certain degree of toxic effect on the cerebral antioxidant system, and the key regulatory factors of cerebral toxicity induced by DLM may still largely unknown. Therefore, it is necessary to elucidate the potential mechanism of DLM-triggered cerebrum injury, and a safe and effective antioxidant for treating DLM-induced organism damage is urgent to be found.

Selenium (Se), a nutritionally essential trace element for humans, acts on mediating varieties of biological protection mechanisms, such as anti-cancer, anti-apoptosis, anti-inflammatory, and improvement of autophagy dysfunction, especially antioxidation [21–25]. Se functionally incorporates into the selenocysteine and then exerts its biological activity through forming various selenoproteins [26, 27]. Also worth noting is that the avian genome encodes 24 selenoproteins [28]. Glutathione peroxidase (GPX) is one of the pivotal antioxidative selenoproteins widely existing in organisms. Concretely, the active center of GPX is selenocysteine, and its activity well reflects the Se level of the body [29]. In homeostasis, GPX composes a component of the antioxidative defense of glutathione (GSH) and plays a fundamental role in eliminating excessive reactive oxygen species (ROS) [30]. During the cellular detoxification of ROS, GPX catalyzes the conversion of GSH to oxidized state-disulfide glutathione (GSSG), and this process involves the decomposition of hydrogen peroxide (carbon dioxide and water as the final products), so as to protect the structure and function of cell membrane from the interference and damage of oxide [31]. GPX4 (phospholipid hydroperoxide GPX) is the key selenoenzyme in GPX family, and each subunit contains one selenocysteine [32]. GPX4 can directly reduce phospholipid and cholesterol hydroperoxides [27]. Previous studies have shown that Se supplementation effectively improved GSH activity, enhanced GPX4 expression, and reduced ROS levels [33]. These results positively provide a basis for the effect of Se as the active center on the activity of GPXs.

In 1957, Se is categorized into the following forms by Schwarz and Foltz: elemental Se, inorganic Se, and organic Se [34]. Among them, elemental Se is poor to be absorbed by organisms [35]. Inorganic Se and organic Se are two sources of dietary Se in animal husbandry [36]. It is worth mentioning that organic Se forms have higher absorption and bioavailability, and more significant biochemical and physiological benefits in animal tissues compared with inorganic Se [37]. This is because inorganic Se may form insoluble complexes in the intestine by recombing with other nutrients, thus reducing the absorption of Se, whereas organic Se can be absorbed faster and higher [38]. Study reported that organic Se (feed with corn–soy-based diets added with 0.15 mg/kg of Se from selenomethionine or Se-enriched yeast) dramatically increased ($p < 0.05$) cytoplasmic thioredoxin reductase activity in both the kidney and the liver than inorganic Se (sodium selenite), thereby enhancing the body's antioxidant capacity [39]. Organic Se was approved as feed supplement by the US Food and Drug Administration in 2000 [40]. According to reports, the maximum amount of organic Se added to diets for poultry feeding in North America is 0.3 mg/kg, and that is 0.5 mg/kg in Europe [41, 42].

Se yeast (SY) is a common and effective organic form of Se supplement, which is famous for its high selenomethionine content [43]. As described previously, SY may increase the content of GPX, and the activity of catalase and superoxide dismutase (SOD) simultaneously decreases

malondialdehyde (MDA) level, thereby removing free radicals and suppressing lipid peroxidation [44, 45]. SY has been shown to protect against oxidative stress-induced intestinal mucosa disruption [46]. Moreover, SY combined with gum Arabic can effectively ameliorate liver inflammation via inhibiting toll-like receptor 4 (TLR4) [44]. However, it is uncertain whether organic Se (from SY) exerts a protective function against DLM-induced cerebral toxicity.

Accordingly, to verify our hypothesis, the current study was performed to interrogate the therapeutic potential and underlying mechanism of dietary SY on DLM-induced cerebrum damage in quails.

Materials and Methods

Chemicals and Reagents

DLM (25 mg mL^{-1}) was acquired from Nanjing Red Sun Co., Ltd (Nanjing, China). SY (Se content ≥ 3 g/kg) was provided by Bosar Biology Group (Yunnan, China). Assay kits (Jiancheng Bioengineering Institute, Nanjing, China) for GPX, MDA, GSH, and SOD were acquired for evaluating redox homeostasis. RIPA buffer and bicinchoninic acid kits were from Beyotime Biotechnology (Jiangsu, China). Trizol was obtained from Ambion (Foster City, CA, USA). SYBR Green RT-qPCR SuperMix and cDNA synthesis kits were bought from Vazyme Biotech Co., Ltd (Nanjing, China), and 2 × PCR Taq Plus Master Mix with dye were from Applied Biological Materials (Vancouver, Canada). Nuclear extraction kits were acquired from Beyotime Biotechnology (Shanghai, China). DNA marker was acquired from Tiangen Biotech Co., Ltd (Beijing, China). Antibodies against nuclear factor-kappa B (NF-κB) and nuclear factor-erythroid-2-related factor 2 (Nrf2) were obtained from Abcam (Cambridge, UK). Antibody against GPX4 was from Beyotime Biotechnology (Shanghai, China). Antibodies against tumor necrosis factor-alpha (TNF-α) and Lamin B were from Bioss Biotechnology (Beijing, China). The antibody of glyceraldehyde-3-phosphate dehydrogenase (GAPDH) was acquired from Ambion (USA). All secondary antibodies were from ZSGB-BIO (Beijing, China).

Animals

Healthy male quails from Wanjia poultry farm (Harbin, China), 3 weeks age, 85 ± 10 g, were acclimated for 1 week prior to official experiment. Quails were housed under the specific conditions (12-h interval light/dark cycle, 22 ± 2 °C, 55 ± 5% relative humidity) with standard diet and water (ad libitum). The animal protocol was performed under the approbation of the Ethical Committee for Animal Experiments (Northeast Agricultural University, Grant Number: 20190928).

Treatments and Sample Collection

A model of SY intervention DLM-induced cerebrum injury in quails was established. Forty quails were distributed into 4 groups randomly: control, DLM, DLM + SY, SY groups ($n = 10$ per group). The weight of quails before treatment was 101.6 ± 1.497 (mean ± SEM). Control quails were intragastrically injected with physiological saline (0.9%, w/v) and provided with standard diet normally. The DLM group was intragastrically injected with 45 mg kg^{-1} body weight DLM solution once a day with standard diet normally. The DLM + SY group was intragastrically injected with 45 mg kg^{-1} body weight DLM solution once a day and provided standard diet with SY (0.4 mg kg^{-1} SY added in daily standard diet). The SY group was provided standard diet with SY (0.4 mg kg^{-1}, added in standard diet). The composition of the standard diet was listed in Table 1 of the supplementary material. DLM was diluted using 0.9% normal saline as a vehicle. The dosage and mode of administration of DLM and SY are based on previous literature and our pre-experimental results [47, 48]. The treatment period was 12 weeks according to our pervious study [48]. All quails were administered with ether anesthesia 24 h after the last treatment. The blood samples were promptly taken out from vein and collected in a vacuum tube (containing heparin sodium anticoagulant) for hematology analysis [49]. Subsequently, quails were dissected, and cerebrum tissue was frozen in liquid nitrogen and stored at − 80 °C for further assay.

Determination of Blood Index

The blood samples of each quail from 4 groups were collected from jugular vein for measuring white blood cells (WBC) count and red blood cells (RBC) number with a cell counting plate [50].

Determination of Se Concentrations

Five cerebrum samples (about 0.1 g) from each group were collected. And the inductively coupled plasma mass spectrometry (ICP-MS) (Thermo, USA) was carried out for analyzing Se concentrations. According to the conventional method described previously [51, 52], cerebrums were added to 5 mL HNO$_3$ for digestion procedure in a microwave system (Anton Paar MW3000, Anton Paar GmbH). Specifically, the samples were digested at 800 W with 190 °C for 5 min, followed by 1400 W with 190 °C for 20 min under 38 MKPa. Then the clarified and transparent filtrates were diluted to 10 mL with

Table 1 Primers sequences for qRT-PCR

Gene	GenBank number	Primer sequence (5′→3′)	Product size (bp)
GPX4	XM_015886371.2	Forward: AAAGCCTTTGCGGAGGGTTACG	103
		Reverse: GCTGCTCCTTCATCCACTTCCAC	
Nrf2	KT151949.1	Forward: GACATGGACAGTTCTCCTGGAAGC	99
		Reverse: GGATAGAGCCTCCGATCCAGACAG	
HO-1	XM_015863488.1	Forward: GCTGAAGAAAATCGCCCAA	107
		Reverse: ATCTCAAGGGCATTCATTCGG	
NQO1	XM_015874306.1	Forward: TATGAGATGGAGACGGCGCA	162
		Reverse: GAAAACGCGGTCAAACCAGC	
TLR4	XM_015878841	Forward: CATCCCAACCCAACCACAGTAGCA	115
		Reverse: TGAGCAGCACCAACGAGTAGTATAGC	
NF-κB	XM_015871827.1	Forward: GCTTCATCCGCCGCCACATC	121
		Reverse: TCCATGACCTGCGAGCCATACC	
TNF-α	XM_015849981	Forward: AGCTGGCGAAGACGGTGGTC	127
		Reverse: TTCGCTGTTAGGTGACGCTGAATG	
COX-2	XM_015869891	Forward: CCTATTACACAAGAAGCCTTCCACCAA	116
		Reverse: TCGCAGCAAGAATTTCTCCACAATCA	
iNOS	XM_015881060	Forward: CTAAGCAAGAAGCAGATACCGATGTCA	164
		Reverse: GCTGTCAGGTGTAATGTGTCAAGAAGG	
JNK3	XM_015861684.2	Forward: GCGAATGTCCTACCTGCTGTATCAA	189
		Reverse: CGAGTCACTACATAAGGCGTCATCAT	
Bax	XM_015869068	Forward: TGCCAGCATGTACCGGACTA	181
		Reverse: GGAGAGGACGATGACCGTGA	
Bcl-2	XM_015854617	Forward: CATTGCCACCTGGATGACCGAGTA	107
		Reverse: GCCTCATACTGTTGCCGTACAATTCC	
Caspase 3	XM_015861411	Forward: ATTGAAGCAGACAGCGGACCAGAT	102
		Reverse: CCAGGAGTAATAGCCAGGAGCAGTAG	
β-actin	XM_015876619.1	Forward: CAGGATGCAGAAGGAGATCACAGC	104
		Reverse: GGATAGAGCCTCCGATCCAGACAG	

deionized water finally used for ICP-MS analysis. The measurement of Se was analyzed based on a standard curve.

Oxidative Stress Bio-marker Measurement

Cerebrum samples (about 0.1 g) from four groups (8 quails per group) were homogenized in 0.9% normal saline on a high-throughput tissue grinder (Scientz-48L, Ningbo Scientz Biotechnology Co., Ltd, Ningbo, China) at 60 Hz for 3 min [53]. After a centrifugation at 3000 r/min for 15 min at 4 °C, the supernatant was extracted for GPX, SOD, MDA, and GSH test in cerebrum with the corresponding commercial kits, respectively [54]. Assays were performed following the manufacturer's instructions.

Organ Histopathology

Cerebrum samples were fixed in 10% formalin and cut into small pieces of 1–2 mm in thickness and 1 cm in length and width. Then sections were washed for 9 h and dehydrated through graded alcohol series [55]. Subsequently, the slices were embedded in paraffin, cut into 3–4 μm thickness, and put on the slides. After drying for 24 h and dewaxing by a series of steps, the slides were stained with hematoxylin and eosin (H&E). Finally, morphology was scanned by a light microscope (BX-FM, Olympus Corp, Tokyo, Japan) [56].

TUNEL Assay

Cerebrum cellular apoptosis ($n = 5$) was assayed with a terminal deoxynucleotidyl transferase-mediated dUTP nick-end labeling (TUNEL) assay kit. After dewaxed with xylene and graded alcohol series, the paraffin sections were penetrated with protease K for 15 min at room temperature. After washed with PBS, the slices were blocked with 3% H_2O_2-carbinol and rinsed with PBS. Then the slices were treated with TUNEL reaction mixture at 37 °C for 1 h, followed by 3 times PBS washing. The slices were incubated

with converter-POD and rinsed again with PBS. Finally, the slices were stained with 3,3'-Diaminobenzidine for 30 min at room temperature, rinsed with PBS, and followed by mounted under glass coverslip [57]. Finally, the samples were evaluated by a light microscope.

Quantitative Reverse Transcription PCR Assay

Total RNA ($n = 6$) was isolated from cerebrum tissues with Trizol reagent. The concentration of RNA was determined with a spectrophotometry at 260 nm [58]. High-Capacity cDNA Reverse Transcription kits were used to synthesize cDNA following the manufacturer's instructions. The primer sequences were designed by Sangon Biotech (Shanghai, China) and shown in Table 1. The PCR was performed with a 20 μL reaction system. Then the melting curve analysis was performed. Relative mRNA levels were normalized compared to β-actin expression. The PCR procedure was performed as previously described [59]. Relative RNA levels were calculated by the $2^{-\Delta\Delta Ct}$ method. Meanwhile, heatmaps of mRNA expression were performed (https://www.omics tudio.cn/tool/4).

Western Blot Assay

Cerebrum samples (about 50 mg) were separated and adequately lysed in RIPA solution (1 mL, including PMSF) for 30 min on ice. Then the Eppendorf tubes were placed in a centrifugal machine to collect the supernatants at 12,000 rpm. The concentration of protein was tested by a BCA kit (Beyotime Biotechnology, Jiangsu, China) [60]. Equal aliquot of the total proteins from cerebrum issues (4 quails per group) were extracted with the appropriate protein extraction kits following the manufacturer's instructions. The concentrations of proteins were tested using the bicinchoninic acid method. Samples (5 μL) were separated by sodium dodecyl sulfate–polyacrylamide gel electrophoresis and then transferred to polyvinylidene difluoride membranes [61]. Subsequently, all membranes were blocked in 5% nonfat milk plus Tris-buffered saline and 20% Tween 20 (TBST) and incubated with primary antibodies overnight at 4 °C. After this, the blots were washed with TBST, incubated with horseradish peroxidase-conjugated secondary antibodies at 37 °C for 30 min, and finally washed 6 times (10 min each time) with TBST. The bands were then visualized with an enhanced chemiluminescence kit [62]. The internal control is designed as GAPDH and Lamin B.

PPI Analysis

Protein–protein interaction (PPI) network of relative genes was constructed and analyzed using STRING database. The functional interaction networks of *Gallus gallus* and *Mus musculus* were based on the interrelationships of target genes in the database. The networks for above two species may better account for the relationship among related genes in this study [63].

Statistical Analysis

One-way analysis of variance and two-way Student's t-test were used to analyze the data. Data represented mean ± standard error of mean (SEM) and analyzed by SPSS 19.0 software (SPSS, Chicago, IL, USA). A $p < 0.05$ was considered statistically significant.

Results

SY Attenuated DLM-Induced Changes of Hematological Indexes in Quail

According to the result of hematologic test, the number of RBC was decreased under DLM treatment with no significant changes (Fig. 1A, $p > 0.05$), while SY reversed this result to a certain extent (Fig. 1A, $p > 0.05$). Meanwhile, DLM significantly decreased WBC count; however, the suppressive effect of DLM was reversed by SY administration (Fig. 1B, $p < 0.05$). Furthermore, there were no mortalities in quails from control or experimental groups.

SY Attenuated DLM-Induced Changes of Se Content in Quail Cerebrum

As displayed in Fig. 1C, the Se content in the DLM group was decreased, but the difference was not significant compared to the control group (Fig. 1C, $p > 0.05$), while SY treatment effectively attenuated the decrease of Se content induced by DLM in DLM + SY group (Fig. 1C, $p < 0.05$).

SY Attenuated DLM-Induced Changes of Pathology in Quail Cerebrum

To visually observe the protective effect of SY on DLM-treated cerebrum, we evaluated the pathological changes according to the H&E staining (Fig. 2). As shown in Fig. 2, the control and SY groups showed normal cerebrum tissue structures (Fig. 2A and D). DLM-treated cerebrum tissues showed disordered cell arrangement with increased spacing of cells (Fig. 2B). Furthermore, karyopyknosis of nerve cells could be observed (Fig. 2B). However, DLM-induced pathological changes were attenuated under the condition of SY treatment (Fig. 2C).
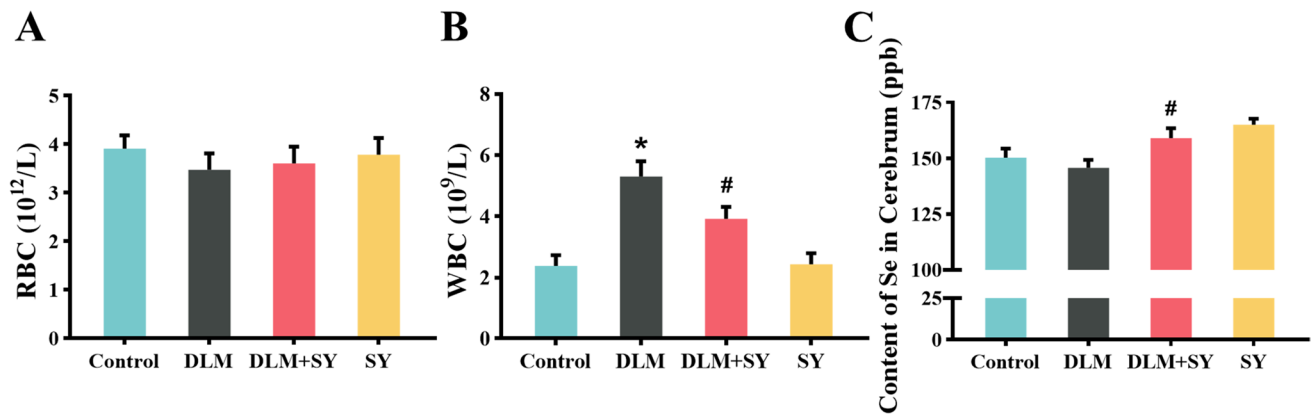
Fig. 1 Effect of SY on hematological changes and Se content induced by DLM in quails. **A** RBC count ($n=10$). **B** WBC count ($n=10$). **C** Content of Se in quail cerebrum ($n=5$). Values are presented as mean $\pm$ SEM. *Significantly different ($p<0.05$) vs. control group; #significantly different ($p<0.05$) vs. DLM-treated group

Fig. 2 Effect of SY on cerebrum pathological changes induced by DLM in quails. **A** Control group. **B** DLM group. **C** DLM+SY group. **D** SY group. Yellow stars, disordered cell arrangement. Green stars, increased cell spacing. Red arrows, karyopyknosis of nerve cells. (H&E staining, magnification 200×)
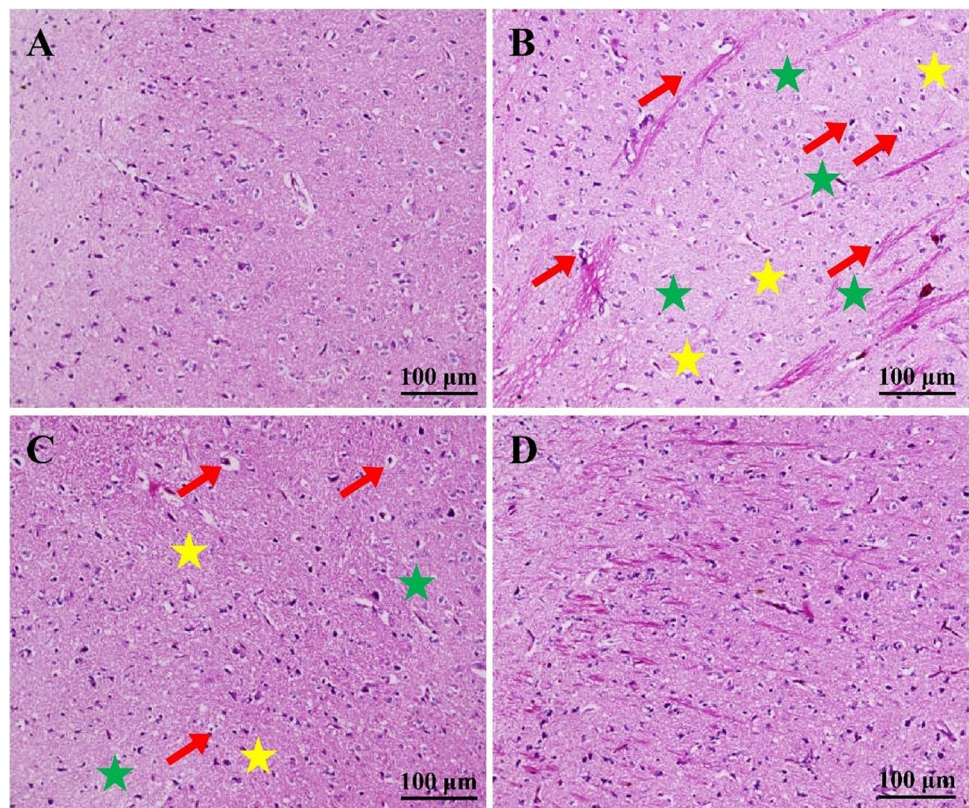
SY Attenuated DLM-Induced Ultrastructure Alteration in Quail Cerebrum

Transmission electron microscope was further used to assess the pathological changes of cerebrum induced by DLM (Fig. 3). The control and SY groups showed normal mitochondria structure (Fig. 3A and D). In the DLM group, severe pathological changes could be frequently observed including mitochondrial swelling, fragmented mitochondrial cristae, and vacuolization of mitochondria (Fig. 3B). Markedly, these pathological changes in the DLM + SY group were less severe than those in the DLM group (Fig. 3C).

SY Changed Redox Homeostasis in Quail Cerebrum Treated by DLM

To further evaluate the redox homeostasis interfered by SY, oxidative stress indices including GPX, SOD, GSH,

Fig. 3 Effect of SY on cerebrum ultrastructural changes induced by DLM in quails. **A** Control group. **B** DLM group. **C** DLM + SY group. **D** SY group. Red arrows, swollen mitochondria. Green arrows, fragmented mitochondrial cristae. Yellow arrows, vacuolization of mitochondria. (Scale bar = 1 μm, magnification 20,000×)
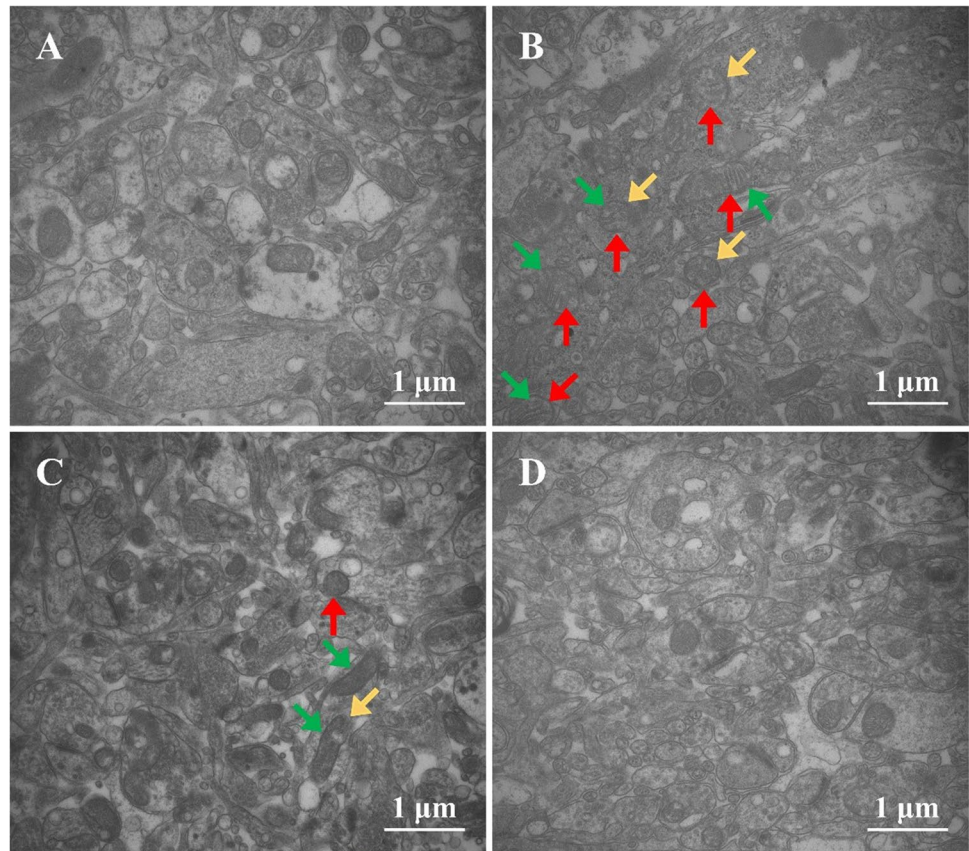
and MDA were tested, respectively. The decreased GPX and SOD activities were shown in DLM-treated group. While in DLM plus SY cotreatment group, the activities of these two enzymes were increased ($p < 0.05$, Fig. 4A

and B). MDA concentration, which is considered as the standard to monitor oxidative stress, was significantly increased in cerebrum exposed to DLM compared with control ($p < 0.05$, Fig. 4C). But compared to the DLM

Fig. 4 Effect of SY on oxidative stress indices in quail cerebrum induced by DLM. **A** GPX activity. **B** SOD activity. **C** MDA level. **D** GSH concentration. Values are presented as mean ± SEM, $n = 8$. *Significantly different ($p < 0.05$) vs. control group; #significantly different ($p < 0.05$) vs. DLM group
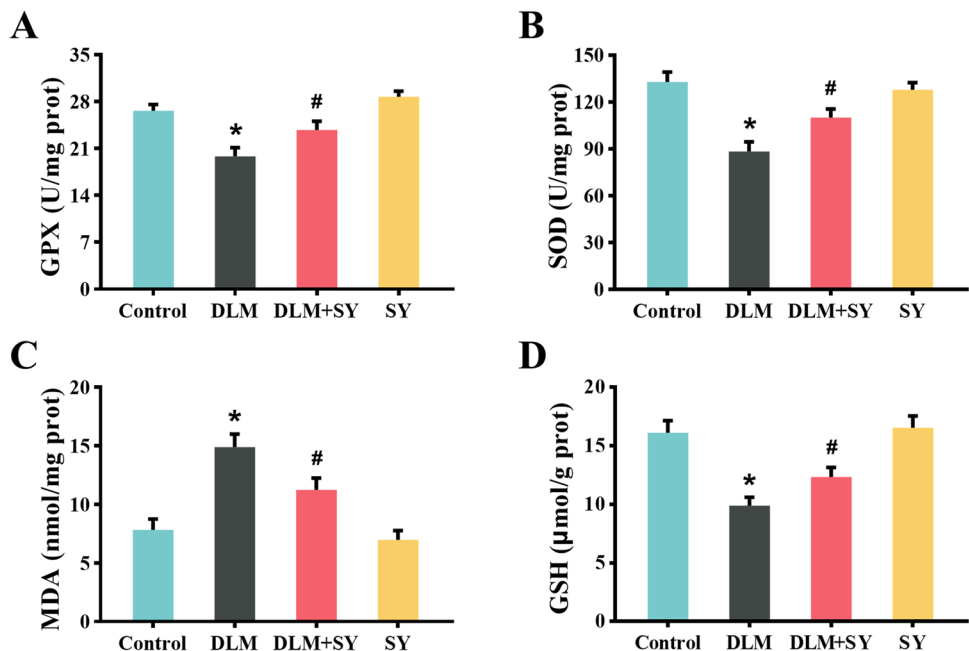
group, MDA level was markedly decreased in DLM plus SY treatment group ($p < 0.05$, Fig. 4C). Similarly, GSH concentration was markedly decreased in DLM-treated groups and treated with SY significantly improved this decrease compared with the control ($p < 0.05$, Fig. 4D).

SY Alleviated GPX4 and Nrf2-Related Redox Homeostasis in DLM-Treated Quail Cerebrum

GPX4 is a member of GPX family and plays a key role in protecting against oxidative stress. The protein level and the mRNA expression of GPX4 were measured, respectively. From Fig. 5A, the protein level of GPX4 was found to be suppressed by DLM, while SY upregulated its level ($p < 0.05$, Fig. 5A). Similarly, the mRNA level change of GPX4 was consistent with GPX4 protein level ($p < 0.05$, Fig. 5B).

To further evaluate whether SY may ameliorate the degree of oxidative stress in quail cerebrum, the levels of Nrf2-related proteins and mRNA expression were examined. The results showed that compared to the control group, the protein level of nuclear Nrf2 and mRNA expression of Nrf2 was significantly downregulated under DLM exposure, but SY supplementation significantly reversed these results ($p < 0.05$, Fig. 5). The downstream mRNA expression of nicotinamide adenine dinucleotide phosphatase: quinone acceptor 1 (NQO1) and heme oxygenase-1 (HO-1) was consistent with the results of Nrf2 ($p < 0.05$, Fig. 5B).

## SY Alleviated TLR4-Associated Inflammation in Quail Cerebrum Induced by DLM

The mRNA levels of inflammation-related genes were detected by qRT-PCR. The mRNA levels of TLR4, NF-κB, TNF-α, inducible nitric oxide synthase (iNOS), and cyclooxygenase-2 (COX-2) were significantly upregulated in DLM-treated group compared with control ($p < 0.05$, Fig. 6B), but co-treated with SY significantly downregulated these changes ($p < 0.05$, Fig. 6B). Moreover, the results of NF-κB and TNF-α protein expression levels were completely consistent with qRT-PCR results ($p < 0.05$, Fig. 6A).

SY Alleviated Apoptosis in Quail Cerebrum Induced by DLM

Imaged and quantified results of TUNEL staining revealed the therapeutic effect of SY on DLM-induced neuronal apoptosis. DLM exposure dramatically increased the ratio of neuronal apoptosis compared with control ($p < 0.05$, Fig. 7A and B). Notably, SY supplementation reversed this growing tendency in the DLM + SY group, indicating that SY significantly restrained DLM-induced apoptosis ($p < 0.05$, Fig. 7B).

To further demonstrate the effect of SY on apoptosis induced by DLM, apoptosis-related proteins and mRNA expression were, respectively, measured by western blot and qRT-PCR. From data, DLM treatment led to a markedly elevation in the mRNA levels of Jun N-terminal kinase 3 (JNK3), caspase 3, and B cell lymphoma gene 2-associated X protein (Bax), but these results were reversed by SY ($p < 0.05$, Fig. 7D). Oppositely, the mRNA expression of

Fig. 5 Effect of SY on GPX4 and Nrf2-related oxidative stress in quail cerebrum induced by DLM. **A** The oxidative stress-related protein level of GPX4 and Nrf2 (nuclear) ($n = 4$). **B** The oxidative stress-related mRNA expression of *GPX4*, *Nrf2*, *NQO1*, and *HO-1* in cerebrum tissues ($n = 6$). Values are presented as mean ± SEM. *Significantly different ($p < 0.05$) vs. control group; #significantly different ($p < 0.05$) vs. DLM group
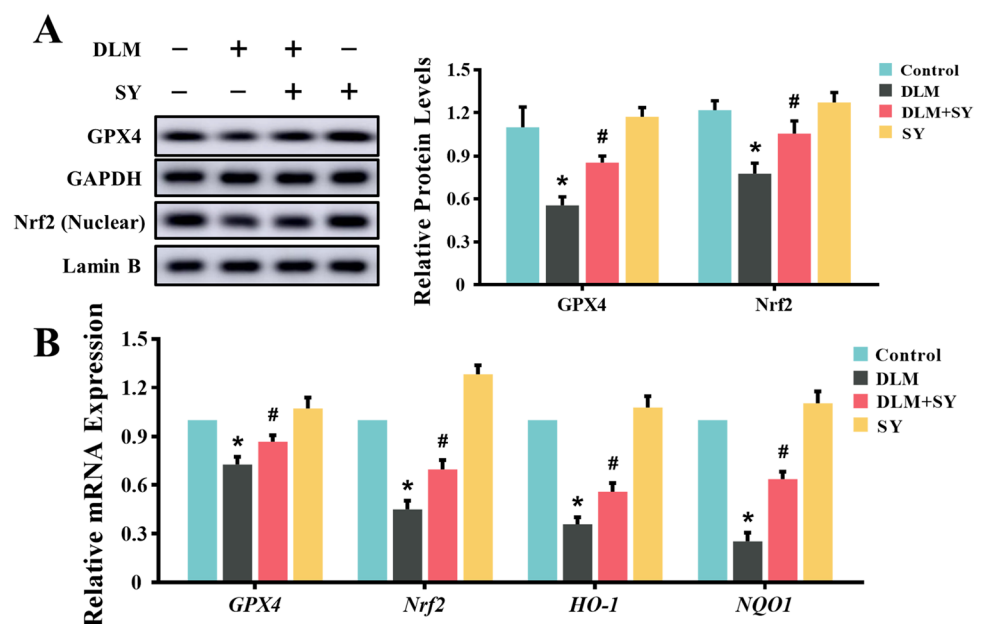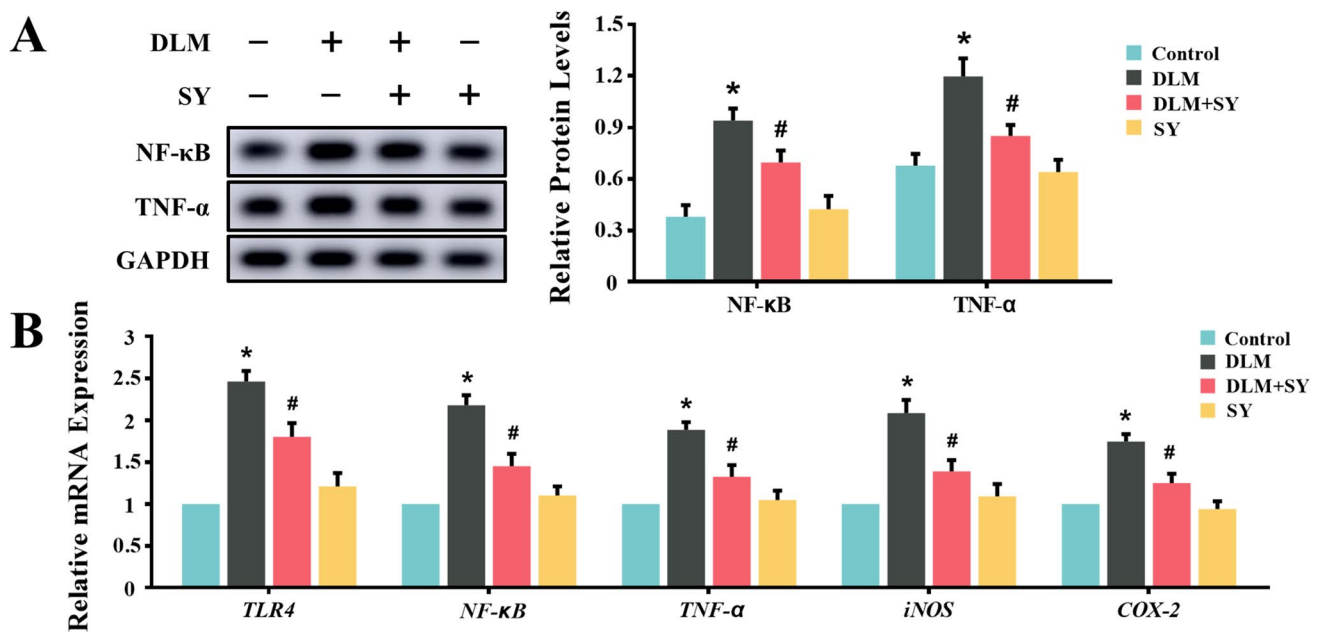
Fig. 6 Effect of SY on TLR4-related inflammation in quail cerebrum induced by DLM. **A** The inflammation-related protein levels of NF-κB and TNF-α in quail cerebrums ($n=4$). **B** The inflammation-related mRNA expression of *TLR4*, *NF-κB*, *TNF-α*, *iNOS*, and *COX-2* in cerebrum ($n=6$). Values are presented as mean ± SEM. *Significantly different ($p < 0.05$) vs. control group; #significantly different ($p < 0.05$) vs. DLM group

B cell lymphoma gene 2 (Bcl-2) was just contrary to the expression results of the above indicators ($p < 0.05$, Fig. 7D). The trend of western blot results including caspase 3, Bax, and Bcl-2 was the same as those of qRT-PCR ($p < 0.05$, Fig. 7C).

Bioinformatics Analysis

The clustering analysis heatmaps and PPI network of genes associated with this study were revealed to demonstrate our hypothesis (Fig. 8A and B). The expression levels of all genes in each group were shown in Fig. 8A, indicating that the oxidative stress (GPX4, Nrf2, HO-1, and NQO1), inflammation (TLR4, NF-κB, TNF-α, iNOS, and COX-2), and apoptosis (JNK3, Caspase 3, Bax, and Bcl-2) related genes were affected by DLM and/or SY administration. As shown in Fig. 8B, the dynamic clusters including GPX1, GPX4, Nrf2, HO-1, NQO1, Keap1, TLR4, COX-2, TNF-α, Caspase 3, JNK3, and Bcl-2 were indicated on the diagram. The functional interaction network revealed the close relationship of the above genes.

Discussion

Pesticide residues in the environment caused by excessive use of DLM have gradually become the focus of ecotoxicology research, so it is necessary to explore the exact

mechanism of its potential toxicity. DLM can be absorbed by organisms through the respiratory tract and digestive tract or via the dermal route causing toxicity to the organism [64–66]. Although studies have interrogated DLM toxicity in some organs, the toxic mechanism of DLM-induced cerebrum damage is poorly understood, and there is a lack of effective therapeutic drugs. Se, a micro-mineral, is a central component of the important active ingredient of selenoprotein GPX, playing a key role in protecting against oxidative stress [28]. The present study firstly reveals that Se from SY effectively attenuates cerebral injury triggered by chronic DLM treatment.

In this study, the negative influence of DLM on the change of histopathology including disordered cell arrangement, increased the spacing of cells spacing, and karyopyknosis of neuron could be visibly observed. Strikingly, SY administration relieved cerebrum injury exposed to DLM. Moreover, SY treatment effectively elevated the Se content in the organisms. And the hematological toxicity mediated by DLM can be reversed by in the presence of SY, which further suggests the possibility of SY as an effective dietary supplement to alleviate cerebrum injury.

Oxidative stress is one of the pivotal mechanisms of nontarget biological damage caused by DLM [14]. Although cells produce ROS under normal metabolism, the overproduction of ROS can weaken antioxidant defense system [67]. DLM can promote the accumulation of ROS, thereby leading to the damage of normal oxidative metabolism [18,
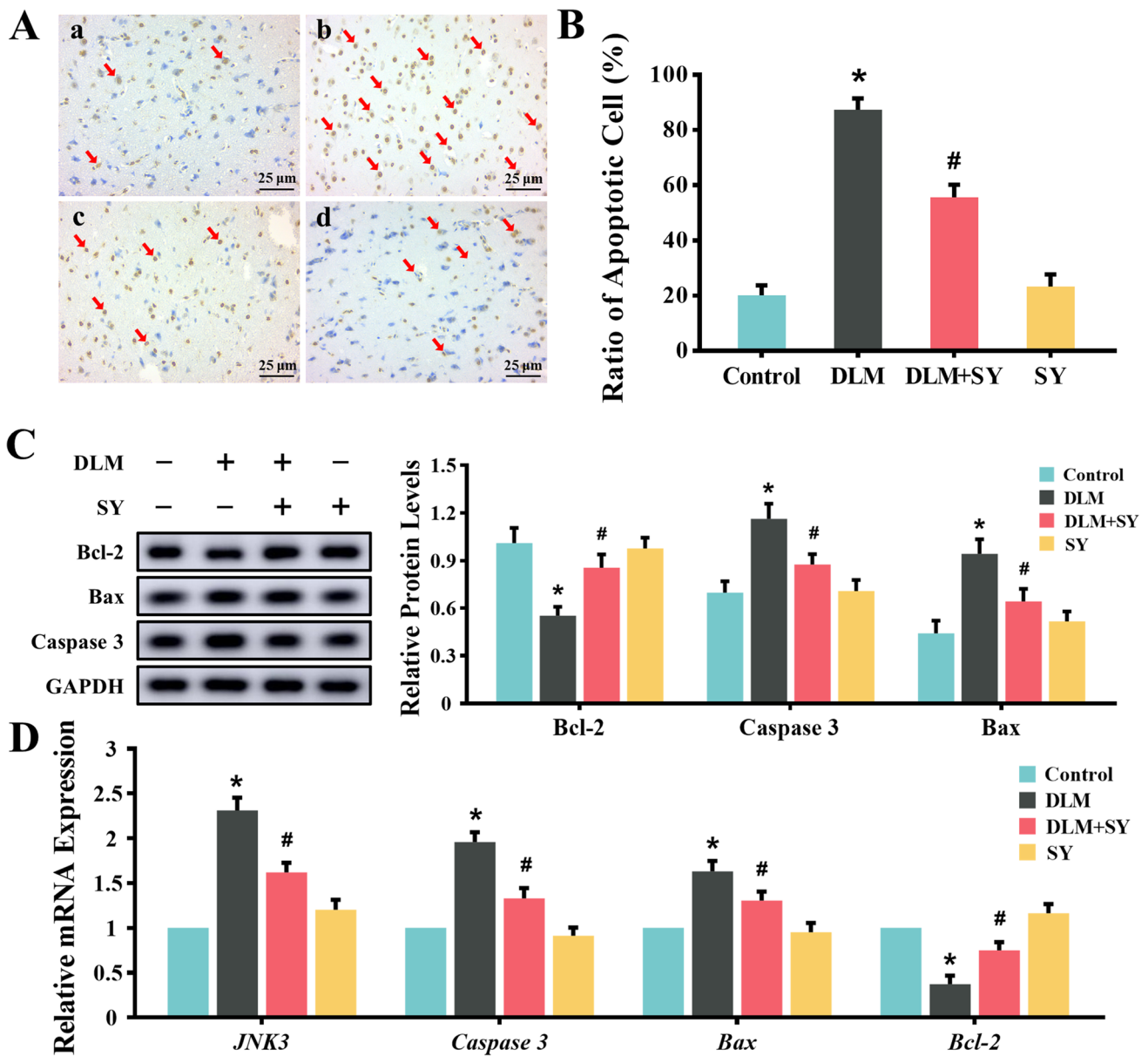
Fig. 7 Effect of SY on DLM-induced apoptosis in quail cerebrum. **A** TUNEL staining (400×magnification; bars=25 μm). **B** Values of quantitative analysis (n=5). **C** The inflammation-related protein levels of Bcl-2, caspase 3, and Bax in cerebrum of quails. Values are presented as mean±SEM (n=4). **D** The apoptosis-related mRNA expression of *JNK3*, *caspase 3*, *Bax*, and *Bcl-2*, in cerebrum of quails (n=6). *Significantly different (p<0.05) vs. control group; #significantly different (p<0.05) vs. DLM group

66]. GPX and SOD are both the pivotal antioxidant enzymes catalyzing the breakdown of ROS [68]. Notably, SY contains the pivotal component of GPX, Se, acted on catalyzing the conversion of reduced GSH into oxidized GSH–GSSG and converting toxic peroxides and organic hydroperoxide into non-toxic hydroxyl compounds, in order to detoxify lipid peroxides and defense against ROS-induced cellular and subcellular oxidative damage, thereby reducing the damage of peroxide to cells [69]. Meanwhile, SOD acts on catalyzing the dismutation of free superoxide to hydrogen peroxide, which was further decomposed to water and GSSG by GPX

[31]. In present study, the suppression of GPX and SOD activities suggested that antioxidant defense system failed to counteract the influx of ROS production induced by chronic DLM exposure. Subsequently, excessive production of ROS attacked the cell membranes and led to lipid peroxidation generating the main products of lipid peroxidation MDA [70]. By contrast, when under the intervention of Se (from SY), the above oxidative stress-related indexes were reversed to a certain extent. In this study, we observed the elevation of GPX and SOD activities, the upregulated level of GSH concentration, and the reduction of MDA in the DLM-treated

Fig. 8 Bioinformatics analysis of related genes expression. **A** Heatmaps of related gene expression. **B** PPI analysis. Protein network of proteins regulated between oxidative stress inflammation-related genes and apoptosis-related genes expressed in the *Gallus gallus* and *Mus musculus* species. GPX1 (Gpx1), GPX4 (Gpx4), Nrf2 (NFE2L2, Nfe2l2), HO-1 (HMOX1, Hmox1), NQO1 (Nqo1), TLR4 (Tlr4), TNF-α (Tnf), COX-2 (Ptgs2), JNK3 (MAPK10, Mapk10), caspase 3 (CASP3, Casp3), Bcl-2 (BCL2, Bcl2)
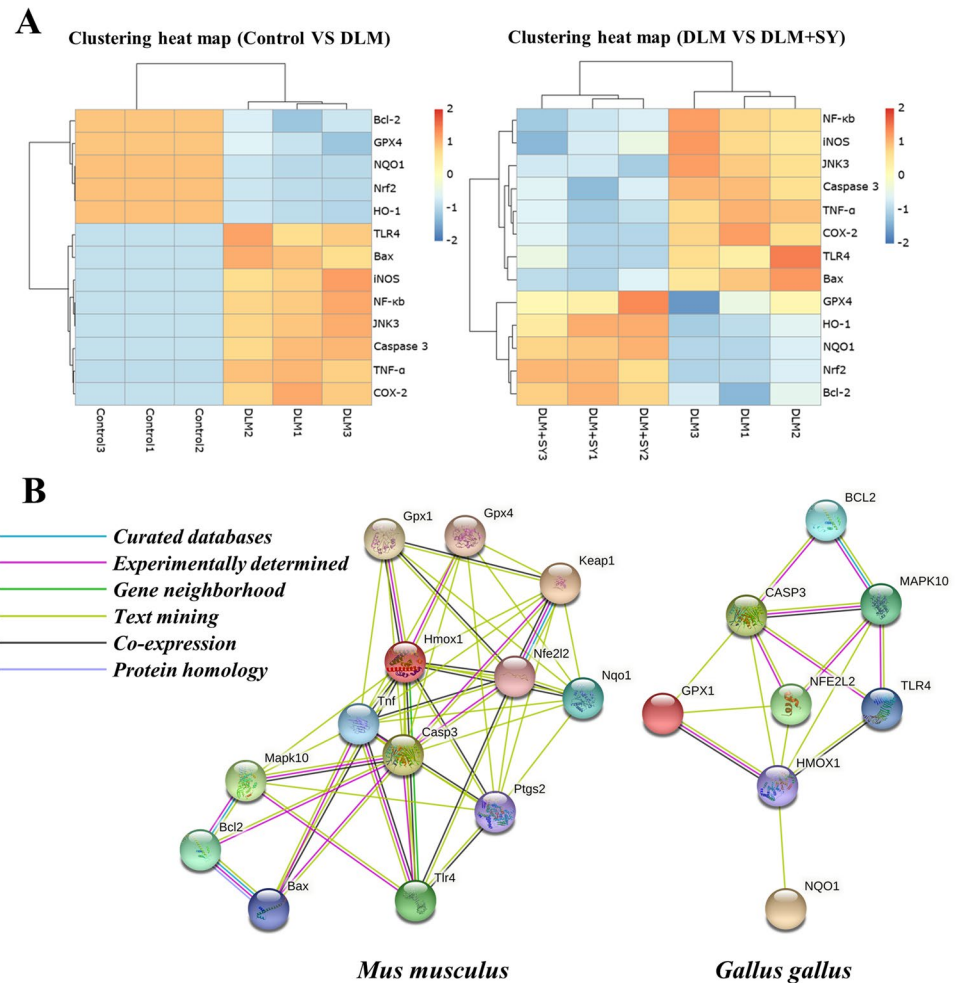

cerebrum. Meanwhile, we found that the GPX4 expression level was elevated under SY administration, indicating that SY enhances the antioxidant enzyme defense system and contributes to correct the imbalance between oxidation and antioxidation, thereby protecting cerebrum against DLM. Further analysis revealed the possibility of GPX4 as a target for the treatment of DLM-induced cerebral injury.

Nrf2 is a key redox sensitive transcription factor, which plays a vital role in defending against various kinds of toxic-induced oxidative stress damage, and is widely distributed in various tissues and organs [71–73]. Nrf2 binds to Kelch-like ECH-associated protein 1 (Keap1) and remains inactive status in the cytoplasm under physiological conditions. Subsequently, Nrf2 is stimulated to separate from Keap1 and transferred to the nucleus to bind with Maf [59]. The Nrf2-Maf heterodimers then bind to antioxidant response elements in the promoters of key antioxidant genes inducing the regulation of a series of antioxidant genes and phase II detoxification enzymes (including HO-1 and NQO1) to maintain intracellular redox homeostasis [47, 59, 74]. Moreover, Reszka et al. (2015) confirmed that Keap1 and Nrf2 change with the concentration of Se in plasma, and they are

negatively correlated and positively correlated, respectively [75]. Our data further verify the antioxidant activity of SY and demonstrate that SY protects quail cerebrum from oxidative stress injury induced by DLM, that is, by elevating the expression of Nrf2 and its target gene products.

TLR4 is one of the pattern recognition receptors triggering different inflammatory responses [18]. TLR4 can be suppressed by Nrf2 to alleviate inflammation-associated lung injury, indicating that oxidative stress along with inflammation is closely related to the development of the disease [76]. The activation of TLR4 signaling works depended on the adaptor protein MyD88, further enhancing the signal cascades that stimulate inflammatory-inducing factor NF-κB gene expression [77]. Subsequently, NF-κB is activated and acts on a variety of pro-inflammatory cytokines including TNF-α, COX-2, and iNOS [78–80]. TNF-α is a major cytokine participated in systemic inflammatory responses [81, 82]. Meanwhile, COX-2 is well considered as a precipitating factor of neuroinflammation in the brain, often used to evaluate the level of brain inflammation [83]. COX-2 and iNOS are both inflammatory proteins that are expressed when microglia are stimulated and activated, suggesting inflammatory responses [84]. The

Fig. 9 Schematic diagram of the mechanism of SY attenuating DLM-induced cerebral injury. SY attenuates DLM-induced cerebral injury in quails via activation of the GPX4/TLR4 signaling pathway
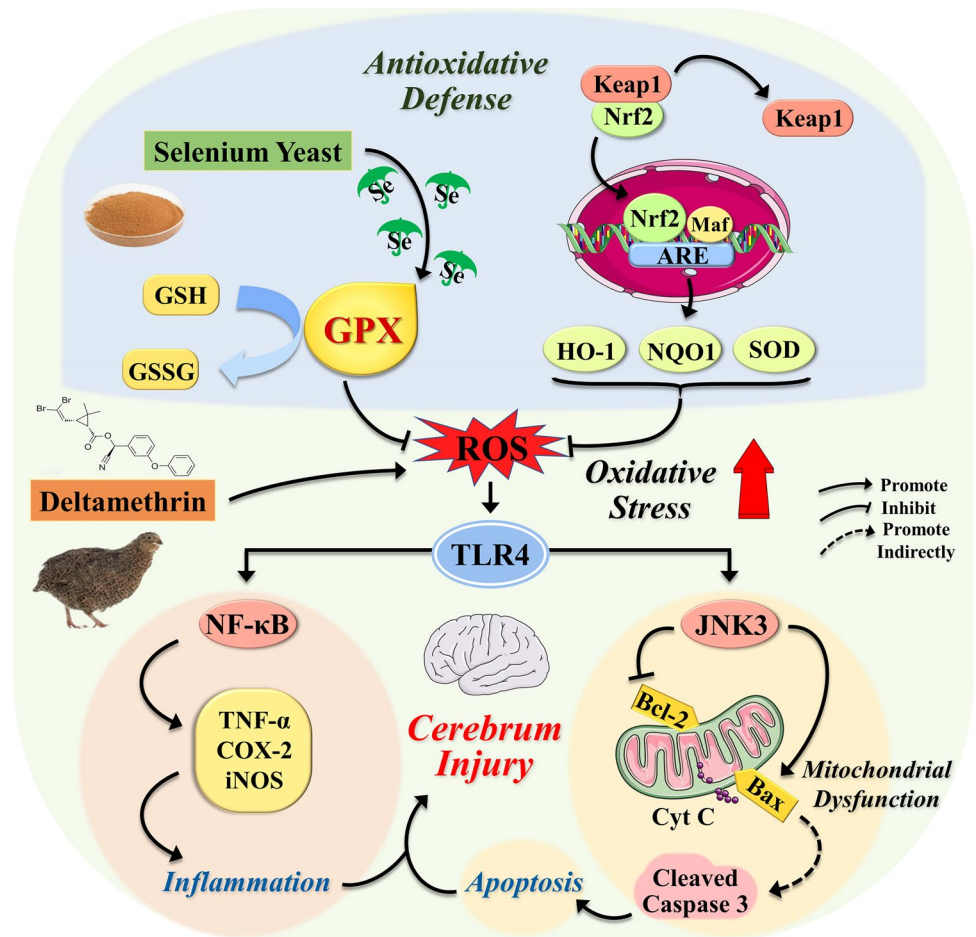
anti-inflammatory mechanism of Se is mainly based on its signal transduction regulation effect on target cells. In vivo experiments have demonstrated that the increase of Se level can suppress NF-κB activation through the catalysis of GPX [85]. Se supplementation can reduce the gene expression of the main pro-inflammatory factors TNF-α and COX-2 via inhibiting the mitogen-activated protein kinase signal pathway [86, 87]. In our study, the alterations in inflammation-related genes and proteins in quails indicate that SY treatment significantly promotes Nrf2 expression and then inhibits the activation of TLR4 and further downregulates inflammatory factor TNF-α, COX-2, and iNOS. Moreover, the increasing trend of WBC was dramatically reversed under SY administration, revealing the protective effect of SY in immune and defense system of organisms. Therefore, our study suggests that SY may effectively protect the quail cerebrum against DLM exposure-induced inflammatory damage to a certain extent via regulating TLR4/NF-κB pathway.

The excessive production of ROS caused by oxidative stress is also one of the mediators of apoptosis pathway [88]. Pervious study announced that TLR-related pathways can be triggered by ROS to lead to cardiomyocyte apoptosis [89]. Of note, Se has been demonstrated to attenuate high

glucose-induced apoptosis of rat cardiomyocytes via suppressing the ROS/TLR4 pathway [90]. JNK3, a member of the JNK family, has been identified to be significantly active and highly expressed in the brain [91]. Under pathological conditions, TLR4 activates JNK3 and then causes the imbalance of apoptosis regulation, which is manifested by downregulating anti-apoptotic protein Bcl-2 and upregulating pro-apoptotic protein Bax [92–94]. Bax enhances the permeability of mitochondrial outer membrane, thereby leading to excessive release of cytochrome c and caspase 3 activation [72, 95]. The activation of caspase 3 subsequently participates in various apoptotic pathway, finally resulting in cell apoptosis [96]. Hence, our study suggests that exogenous addition of SY effectively alleviates DLM-induced apoptosis in quail cerebrum involved in the activation of TLR4 pathway. Taken together, the organic Se supplement through SY raises hopes that the amelioration in DLM-induced cerebral toxicity may be possible, and the positive regulation of GPX4 on antioxidative defense is considered as the main therapeutic target of Se administration for treating cerebrum injury. In summary, this study suggests that activation of the GPX4/TLR4 is primarily involved in the cerebrum injury induced by chronic DLM exposure (Fig. 9).

Conclusion

Herein, our study demonstrates that SY attenuates DLM-induced cerebrum injury in quails via activation of the GPX4/TLR4 signaling pathway. GPX4 may be an effective therapeutic target for the treatment of DLM-induced cerebral injury. Furthermore, this study not only provides a novel insight for elucidating DLM-induced cerebrum toxicity, but also a practical foundation for the treatment of DLM-induced damage by dietary supplement of SY.

Data Availability The datasets generated during and/or analyzed during the current study are available from the corresponding author on reasonable request.

Declarations

Ethics Approval The animal protocol was performed under the approbation of the Ethical Committee for Animal Experiments (Northeast Agricultural University, Grant Number: 20190928).

Consent to Participate Not applicable.

Consent for Publication All authors provide consent for publication.

Conflict of Interest The authors declare no competing interests.

References

1. Braguini WL, Cadena SM, Carnieri EG, Rocha ME, de Oliveira MB (2004) Effects of deltamethrin on functions of rat liver mitochondria and on native and synthetic model membranes. Toxicol Lett 152:191–202. https://doi.org/10.1016/j.toxlet.2004.03.017

2. Guardiola FA, Gónzalez-Párraga P, Meseguer J, Cuesta A, Esteban MA (2014) Modulatory effects of deltamethrin-exposure on the immune status, metabolism and oxidative stress in gilthead seabream (*Sparus aurata* L.). Fish Shellfish Immunol 36:120–129. https://doi.org/10.1016/j.fsi.2013.10.020

3. Song YF, Kai JR, Song XY, Zhang W, Li LL (2015) Long-term toxic effects of deltamethrin and fenvalerante in soil. J Hazard Mater 289:158–164. https://doi.org/10.1016/j.jhazmat.2015.02.057

4. Brooks SJ, Ruus A, Rundberget JT, Kringstad A, Lillicrap A (2019) Bioaccumulation of selected veterinary medicinal products (VMPs) in the blue mussel (*Mytilus edulis*). Sci Total Environ 655:1409–1419. https://doi.org/10.1016/j.scitotenv.2018.11.212

5. Chandra N, Jain NK, Sondhia S, Srivastava AB (2013) Deltamethrin induced toxicity and ameliorative effect of alpha-tocopherol in broilers. Bull Environ Contam Toxicol 90:673–678. https://doi.org/10.1007/s00128-013-0981-z

6. Dong T, Lin L, He Y, Nie PC, Qu FF, Xiao SP (2018) Density functional theory analysis of deltamethrin and its determination in strawberry by surface enhanced Raman spectroscopy. Molecules 23:1458. https://doi.org/10.3390/molecules23061458

7. Parsons AE, Escobar-Lux RH, Sævik PN, Samuelsen OB, Agnalt AL (2020) The impact of anti-sea lice pesticides, azamethiphos and deltamethrin, on European lobster (*Homarus gammarus*) larvae in the Norwegian marine environment. Environ Pollut 264:114725. https://doi.org/10.1016/j.envpol.2020.114725

8. Richardson JR, Taylor MM, Shalat SL, Guillot TS, Caudle WM, Hossain MM, Mathews TA, Jones SR, Cory-Slechta DA, Miller GW (2015) Developmental pesticide exposure reproduces features of attention deficit hyperactivity disorder. FASEB J 29:1960–1972. https://doi.org/10.1096/fj.14-260901

9. Wu YQ, Li WH, Yuan MR, Liu X (2020) The synthetic pyrethroid deltamethrin impairs zebrafish (*Danio rerio*) swim bladder development. Sci Total Environ 701:134870. https://doi.org/10.1016/j.scitotenv.2019.134870

10. Li M, Liu XY, Feng XZ (2019) Cardiovascular toxicity and anxiety-like behavior induced by deltamethrin in zebrafish (*Danio rerio*) larvae. Chemosphere 219:155–164. https://doi.org/10.1016/j.chemosphere.2018.12.011

11. Liu XY, Gao Q, Feng ZY, Tang YQ, Zhao X, Chen DY, Feng XZ (2021) Protective effects of spermidine and melatonin on deltamethrin-induced cardiotoxicity and neurotoxicity in zebrafish. Cardiovasc Toxicol 21:29–41. https://doi.org/10.1007/s12012-020-09591-5

12. Ning MX, Hao WJ, Cao C, Xie XJ, Fan WF, Huang H, Yue YC, Tang MY, Wang W, Gu W, Meng QG (2020) Toxicity of deltamethrin to *Eriocheir sinensis* and the isolation of a deltamethrin-degrading bacterium, *Paracoccus sp.* P-2. Chemosphere 257:127162. https://doi.org/10.1016/j.chemosphere.2020.127162

13. Osama E, Galal AAA, Abdalla H, El-Sheikh SMA (2019) Chlorella vulgaris ameliorates testicular toxicity induced by deltamethrin in male rats via modulating oxidative stress. Andrologia 51:e13214. https://doi.org/10.1111/and.13214

14. Lu QR, Sun YQ, Ares I, Anadón A, Martínez M, Martínez-Larrañaga MR, Yuan ZH, Wang X, Martinez MA (2019) Deltamethrin toxicity: a review of oxidative stress and metabolism. Environ Res 170:260–281. https://doi.org/10.1016/j.envres.2018.12.045

15. Jia ZZ, Zhang JW, Zhou D, Xu DQ, Feng XZ (2019) Deltamethrin exposure induces oxidative stress and affects meiotic maturation in mouse oocyte. Chemosphere 223:704–713. https://doi.org/10.1016/j.chemosphere.2019.02.092

16. Özdemir S, Altun S, Özkaraca M, Ghosi A, Toraman E, Arslan H (2018) Cypermethrin, chlorpyrifos, deltamethrin, and imidacloprid exposure up-regulates the mRNA and protein levels of bdnf and c-fos in the brain of adult zebrafish (*Danio rerio*). Chemosphere 203:318–326. https://doi.org/10.1016/j.chemosphere.2018.03.190

17. Parlak V (2018) Evaluation of apoptosis, oxidative stress responses, AChE activity and body malformations in zebrafish

(*Danio rerio*) embryos exposed to deltamethrin. Chemosphere 207:397–403. https://doi.org/10.1016/j.chemosphere.2018.05.112

18. Zhang C, Zhang Q, Pang YY, Song XZ, Zhou N, Wang J, He L, Lv JH, Song Y, Cheng Y, Yang XZ (2019) The protective effects of melatonin on oxidative damage and the immune system of the Chinese mitten crab (*Eriocheir sinensis*) exposed to deltamethrin. Sci Total Environ 653:1426–1434. https://doi.org/10.1016/j.scitotenv.2018.11.063

19. Salim S (2017) Oxidative stress and the central nervous system. J Pharmacol Exp Ther 360:201–205. https://doi.org/10.1124/jpet.116.237503

20. Yousof SM, Awad YM, Mostafa EMA, Hosny MM, Anwar MM, Eldesouki RE, Badawy AE (2021) The potential neuroprotective role of Amphora coffeaeformis algae against monosodium glutamate-induced neurotoxicity in adult albino rats. Food Funct 12:706–716. https://doi.org/10.1039/d0fo01957g

21. Balaban H, Nazıroğlu M, Demirci K, Övey İS (2017) The protective role of selenium on scopolamine-induced memory impairment, oxidative stress, and apoptosis in aged rats: the involvement of TRPM2 and TRPV1 channels. Mol Neurobiol 54:2852–2868. https://doi.org/10.1007/s12035-016-9835-0

22. Chung S, Zhou R, Webster TJ (2020) Green synthesized BSA-coated selenium nanoparticles inhibit bacterial growth while promoting mammalian cell growth. Int J Nanomedicine 15:115–124. https://doi.org/10.2147/IJN.S193886

23. Qian F, Misra S, Prabhu KS (2019) Selenium and selenoproteins in prostanoid metabolism and immunity. Crit Rev Biochem Mol Biol 54:484–516. https://doi.org/10.1080/10409238.2020.1717430

24. Reid ME, Duffield-Lillico AJ, Slate E, Natarajan N, Turnbull B, Jacobs E, Combs GFJR, Alberts DS, Clark LC, Marshall JR (2008) The nutritional prevention of cancer: 400 mcg per day selenium treatment. Nutr Cancer 60:155–163. https://doi.org/10.1080/01635580701684856

25. Ren XM, Wang SS, Zhang CQ, Hu XD, Zhou L, Li YH, Xu LC (2020) Selenium ameliorates cadmium-induced mouse Leydig TM3 cell apoptosis via inhibiting the ROS/JNK/c-jun signaling pathway. Ecotoxicol Environ Saf 192:110266. https://doi.org/10.1016/j.ecoenv.2020.110266

26. Bulteau AL, Chavatte L (2015) Update on selenoprotein biosynthesis. Antioxid Redox Signal 23:775–794. https://doi.org/10.1089/ars.2015.6391

27. Lu J, Holmgren A (2009) Selenoproteins. J Biol Chem 284:723–727. https://doi.org/10.1074/jbc.R800045200

28. Nassef E, Saker O, Shukry M (2020) Effect of Se sources and concentrations on performance, antioxidant defense, and functional egg quality of laying Japanese quail (*Coturnix japonica*). Environ Sci Pollut Res Int 27:37677–37683. https://doi.org/10.1007/s11356-020-09853-3

29. Guillin OM, Vindry C, Ohlmann T, Chavatte L (2019) Selenium, selenoproteins and viral infection. Nutrients 11:2101. https://doi.org/10.3390/nu11092101

30. Del Vesco AP, Gasparino E (2013) Production of reactive oxygen species, gene expression, and enzymatic activity in quail subjected to acute heat stress. J Anim Sci 91:582–587. https://doi.org/10.2527/jas.2012-5498

31. Kesheri M, Kanchan S, Richa SRP (2014) Isolation and in silico analysis of Fe-superoxide dismutase in the cyanobacterium Nostoc commune. Gene 553:117–125. https://doi.org/10.1016/j.gene.2014.10.010

32. Ansong E, Yang W, Diamond AM (2014) Molecular cross-talk between members of distinct families of selenium containing proteins. Mol Nutr Food Res 58:117–123. https://doi.org/10.1002/mnfr.201300543

33. Gan F, Xue H, Huang Y, Pan C, Huang K (2015) Selenium alleviates porcine nephrotoxicity of ochratoxin A by improving selenoenzyme expression in vitro. PLoS ONE 10:e0119808. https://doi.org/10.1371/journal.pone.0119808

34. Schwarz K, Foltz CM (1957) Selenium as an integral part of factor 3 against dietary necrotic liver degeneration. J Am Chem Soc 79:3292–3293

35. Ye RH, Huang JQ, Wang ZX, Chen YX, Dong YL (2021) Trace element selenium effectively alleviates intestinal diseases. Int J Mol Sci 22:11708

36. Kim JH, Kil DY (2020) Comparison of toxic effects of dietary organic or inorganic selenium and prediction of selenium intake and tissue selenium concentrations in broiler chickens using feather selenium concentrations. Poult Sci 99:6462–6473. https://doi.org/10.1016/j.psj.2020.08.061

37. Kieliszek M (2019) Selenium-fascinating microelement, properties and sources in food. Molecules 24:1298. https://doi.org/10.3390/molecules24071298

38. Mahima VAK, Kumar A, Rahal A, Kumar V, Roy D (2012) Inorganic versus organic selenium supplementation: a review. Pak J Biol Sci 15:418–425. https://doi.org/10.3923/pjbs.2012.418.425

39. Yuan D, Zhan XA, Wang YX (2012) Effect of selenium sources on the expression of cellular glutathione peroxidase and cytoplasmic thioredoxin reductase in the liver and kidney of broiler breeders and their offspring. Poult Sci 91:936–942. https://doi.org/10.3382/ps.2011-01921

40. Federal Register. Food additives permitted in feed and drinking water of animals; Selenium yeast. https://www.federalregister.gov/documents/2000/06/06/00-14214/food-additives-permitted-in-feed-and-drinking-water-of-animals-selenium-yeast. (accessed Jan. 2020).

41. Food and Drug Administration (FDA) (2003) Food additives permitted in feed and drinking water of animals: Delenium yeast. Federal Register 68:52339–52340

42. Ibrahim D, Kishawy ATY, Khater SI, Hamed Arisha AH, Mohammed HA, Abdelaziz AS, Abd El-Rahman GI, Elabbasy MT (2019) Effect of dietary modulation of selenium form and level on performance, tissue retention, quality of frozen stored meat and gene expression of antioxidant status in ross broiler chickens. Animals (Basel) 9:342. https://doi.org/10.3390/ani9060342

43. Zhang ZH, Wu QY, Chen C, Zheng R, Chen Y, Ni JZ, Song GL (2018) Comparison of the effects of selenomethionine and selenium-enriched yeast in the triple-transgenic mouse model of Alzheimer's disease. Food Funct 9:3965–3973. https://doi.org/10.1039/c7fo02063e

44. Hamid M, Abdulrahim Y, Liu D, Qian G, Khan A, Huang K (2018) The hepatoprotective effect of selenium-enriched yeast and gum arabic combination on carbon tetrachloride-induced chronic liver injury in rats. J Food Sci 83:525–534. https://doi.org/10.1111/1750-3841.14030

45. Wang XD, Shen ZH, Wang CL, Li EC, Qin JG, Chen LQ (2019) Dietary supplementation of selenium yeast enhances the antioxidant capacity and immune response of juvenile *Eriocheir Sinensis* under nitrite stress. Fish Shellfish Immunol 87:22–31. https://doi.org/10.1016/j.fsi.2018.12.076

46. Liu L, Wu CM, Chen DW, Yu B, Huang ZQ, Luo YH, Zheng P, Mao XB, Yu J, Luo JQ, Yan H, He J (2020) Selenium-enriched yeast alleviates oxidative stress-induced intestinal mucosa disruption in weaned pigs. Oxid Med Cell Longev 2020:5490743. https://doi.org/10.1155/2020/5490743

47. Li P, Li K, Zou C, Tong C, Sun L, Cao ZJ, Yang SH, Lyu QF (2020) Selenium yeast alleviates ochratoxin a-induced hepatotoxicity via modulation of the PI3K/AKT and Nrf2/Keap1 signaling pathways in chickens. Toxins (Basel) 12:143. https://doi.org/10.3390/toxins12030143

48. Han B, Lv ZJ, Zhang XY, Lv YY, Li SY, Wu PF, Yang QY, Li JY, Qu B, Zhang ZG (2020) Deltamethrin induces liver fibrosis in quails via activation of the TGF-β1/Smad signaling pathway.

Environ Pollut 259:113870. https://doi.org/10.1016/j.envpol.2019.113870

49. Yang DQ, Lv ZJ, Zhang HL, Liu BY, Jiang HJ, Tan X, Lu JJ, Baiyun RQ, Zhang ZG (2017) Activation of the Nrf2 signaling pathway involving KLF9 plays a critical role in allicin resisting against arsenic trioxide-induced hepatotoxicity in rats. Biol Trace Elem Res 176:192–200. https://doi.org/10.1007/s12011-016-0821-1

50. Lv YY, Bing QZ, Lv ZJ, Xue JD, Li SY, Han B, Yang QY, Wang XQ, Zhang ZG (2020) Imidacloprid-induced liver fibrosis in quails via activation of the TGF-β1/Smad pathway. Sci Total Environ 705:135915. https://doi.org/10.1016/j.scitotenv.2019.135915

51. Barbosa V, Maulvault AL, Anacleto P, Santos M, Mai M, Oliveira H, Delgado I, Coelho I, Barata M, Araújo-Luna R, Ribeiro L, Eljasik P, Sobczak M, Sadowski J, Tórz A, Panicz R, Dias J, Pousão-Ferreira P, Carvalho ML, Martins M, Marques A (2021) Effects of steaming on health-valuable nutrients from fortified farmed fish: gilthead seabream (*Sparus aurata*) and common carp (*Cyprinus carpio*) as case studies. Food Chem Toxicol 152:112218. https://doi.org/10.1016/j.fct.2021.112218

52. Delgado I, Ventura M, Gueifão S, Coelho I, Nascimento AC, Silva JAL, Castanheira I (2019) 12th IFDC 2017 special issue–iodine, selenium and iron contents in Portuguese key foods as consumed. J Food Compos Anal 79:39–46. https://doi.org/10.1016/j.jfca.2019.03.004

53. Li JY, Zheng XY, Ma XY, Xu XY, Du Y, Lv QJ, Li XR, Wu Y, Sun HX, Yu LJ, Zhang ZG (2019) Melatonin protects against chromium(VI)-induced cardiac injury via activating the AMPK/Nrf2 pathway. J Inorg Biochem 197:110698. https://doi.org/10.1016/j.jinorgbio.2019.110698

54. Li SY, Baiyun RQ, Lv ZJ, Li JY, Han DX, Zhao WY, Yu LJ, Deng N, Liu ZY, Zhang ZG (2019) Exploring the kidney hazard of exposure to mercuric chloride in mice: disorder of mitochondrial dynamics induces oxidative stress and results in apoptosis. Chemosphere 234:822–829. https://doi.org/10.1016/j.chemosphere.2019.06.096

55. Lu JJ, Jiang HJ, Liu BY, Baiyun RQ, Li SY, Lv YY, Li D, Qiao SQ, Tan X, Zhang ZG (2018) Grape seed procyanidin extract protects against Pb-induced lung toxicity by activating the AMPK/Nrf2/p62 signaling axis. Food Chem Toxicol 116:59–69. https://doi.org/10.1016/j.fct.2018.03.034

56. Zheng XY, Li SY, Li JY, Lv YY, Wang XQ, Wu PF, Yang QY, Tang YQ, Liu Y, Zhang ZG (2020) Hexavalent chromium induces renal apoptosis and autophagy via disordering the balance of mitochondrial dynamics in rats. Ecotoxicol Environ Saf 204:11061. https://doi.org/10.1016/j.ecoenv.2020.111061

57. Li SY, Zheng XY, Zhang XY, Yu HX, Han B, Lv YY, Liu Y, Wang XQ, Zhang ZG (2021) Exploring the liver fibrosis induced by deltamethrin exposure in quails and elucidating the protective mechanism of resveratrol. Ecotoxicol Environ Saf 207:111501. https://doi.org/10.1016/j.ecoenv.2020.111501

58. Han BQ, Lv ZJ, Han XM, Li SY, Han B, Yang QY, Wang XQ, Wu PF, Li JY, Deng N, Zhang ZG (2022) Harmful effects of inorganic mercury exposure on kidney cells: Mitochondrial dynamics disorder and excessive oxidative stress. Biol Trace Elem Res 200:1591–1597. https://doi.org/10.1007/s12011-021-02766-3

59. Han B, Li SY, Lv YY, Yang DQ, Li JY, Yang QY, Wu PF, Lv ZJ, Zhang ZG (2019) Dietary melatonin attenuates chromium-induced lung injury via activating the Sirt1/Pgc-1α/Nrf2 pathway. Food Funct 10:5555–5565. https://doi.org/10.1039/c9fo01152h

60. Li SY, Han B, Wu PF, Yang QY, Wang XQ, Li JY, Liao YG, Deng N, Jiang HJ, Zhang ZG (2022) Effect of inorganic mercury exposure on reproductive system of male mice: immunosuppression and fibrosis in testis. Environ Toxicol 37:69–78. https://doi.org/10.1002/tox.23378

61. Han B, Wang XQ, Wu PF, Jiang HJ, Yang QY, Li SY, Li JY, Zhang ZG (2021) Pulmonary inflammatory and fibrogenic response induced by graphitized multi-walled carbon nanotube involved in cGAS-STING signaling pathway. J Hazard Mater 417:125984. https://doi.org/10.1016/j.jhazmat.2021.125984

62. Yang DQ, Jiang HJ, Lu JJ, Lv YY, Baiyun RQ, Li SY, Liu BY, Lv ZJ, Zhang ZG (2018) Dietary grape seed proanthocyanidin extract regulates metabolic disturbance in rat liver exposed to lead associated with PPARα signaling pathway. Environ Pollut 237:377–387. https://doi.org/10.1016/j.envpol.2018.02.035

63. Yang QY, Han B, Li SY, Wang XQ, Wu PF, Liu Y, Li JY, Han BQ, Deng N, Zhang ZG (2022) The link between deacetylation and hepatotoxicity induced by exposure to hexavalent chromium. J Adv Res 35:129–140. https://doi.org/10.1016/j.jare.2021.04.002

64. Hołyńska-Iwan I, Szewczyk-Golec K (2020) Pyrethroids: how they affect human and animal health? Medicina (Kaunas) 56:582. https://doi.org/10.3390/medicina56110582

65. Hołyńska-Iwan I, Bogusiewicz J, Chajdas D, Szewczyk-Golec K, Lampka M, Olszewska-Słonina D (2018) The immediate influence of deltamethrin on ion transport through rabbit skin. An in vitro study. Pestic Biochem Physiol 148:144–150. https://doi.org/10.1016/j.pestbp.2018.04.011

66. Su LJ, Zhang JH, Gomez H, Murugan R, Hong X, Xu D, Jiang F, Peng ZY (2019) Reactive oxygen species-induced lipid peroxidation in apoptosis, autophagy, and ferroptosis. Oxid Med Cell Longev 2019:5080843

67. Anstee QM, Goldin RD (2006) Mouse models in non-alcoholic fatty liver disease and steatohepatitis research. Int J Exp Pathol 87:1–16. https://doi.org/10.1111/j.0959-9673.2006.00465.x

68. Matović V, Buha A, Đukić-Ćosić D, Bulat Z (2015) Insight into the oxidative stress induced by lead and/or cadmium in blood, liver and kidneys. Food Chem Toxicol 78:130–140. https://doi.org/10.1016/j.fct.2015.02.011

69. Takata N, Myburgh J, Botha A, Nomngongo PN (2021) The importance and status of the micronutrient selenium in South Africa: a review. Environ Geochem Health. https://doi.org/10.1007/s10653-021-01126-3

70. Tsikas D (2017) Assessment of lipid peroxidation by measuring malondialdehyde (MDA) and relatives in biological samples: analytical and biological challenges. Anal Biochem 524:13–30. https://doi.org/10.1016/j.ab.2016.10.021

71. Liu BY, Jiang HJ, Lu JJ, Baiyun RQ, Li SY, Lv YY, Li D, Wu H, Zhang ZG (2018) Grape seed procyanidin extract ameliorates lead-induced liver injury via miRNA153 and AKT/GSK-3β/Fyn-mediated Nrf2 activation. J Nutr Biochem 52:115–123. https://doi.org/10.1016/j.jnutbio.2017.09.025

72. Song C, Heping HF, Shen YS, Jin SX, Li DY, Zhang AG, Ren XL, Wang KL, Zhang L, Wang JD, Shi DM (2020) AMPK/p38/Nrf2 activation as a protective feedback to restrain oxidative stress and inflammation in microglia stimulated with sodium fluoride. Chemosphere 244:125495. https://doi.org/10.1016/j.chemosphere.2019.125495

73. Wang XQ, Han B, Wu PF, Li SY, Lv YY, Lu JJ, Yang QY, Li JY, Zhu Y, Zhang ZG (2020) Dibutyl phthalate induces allergic airway inflammation in rats via inhibition of the Nrf2/TSLP/JAK1 pathway. Environ Pollut 267:115564. https://doi.org/10.1016/j.envpol.2020.115564

74. Lv YY, Jiang HJ, Li SY, Han B, Liu Y, Yang DQ, Li JY, Yang QY, Zhang WuPF, ZG, (2020) Sulforaphane prevents chromium-induced lung injury in rats via activation of the Akt/GSK-3β/Fyn pathway. Environ Pollut 259:113812. https://doi.org/10.1016/j.envpol.2019.113812

75. Reszka E, Wieczorek E, Jablonska E, Janasik B, Fendler W, Wasowicz W (2015) Association between plasma selenium level and NRF2 target genes expression in humans. J Trace Elem Med Biol 30:102–106. https://doi.org/10.1016/j.jtemb.2014.11.008

76. Yan J, Li JJ, Zhang L, Sun Y, Jiang J, Huang Y, Xu H, Jiang H, Hu R (2018) Nrf2 protects against acute lung injury and inflammation

by modulating TLR4 and Akt signaling. Free Radic Biol Med 121:78–85. https://doi.org/10.1016/j.freeradbiomed.2018.04.557

77. Vilahur G, Badimon L (2014) Ischemia/reperfusion activates myocardial innate immune response: the key role of the toll-like receptor. Front Physiol 5:496. https://doi.org/10.3389/fphys.2014.00496

78. Choe U, Li YF, Yu L, Gao BY, Wang TTY, Sun JH, Chen P, Yu LL (2020) Chemical composition of cold-pressed blackberry seed flour extract and its potential health-beneficial properties. Food Sci Nutr 8:1215–1225. https://doi.org/10.1002/fsn3.1410

79. Zhang ZG, Guo CM, Jiang HJ, Han B, Wang XQ, Li SY, Lv YY, Lv ZJ, Zhu Y (2020) Inflammation response after the cessation of chronic arsenic exposure and post-treatment of natural astaxanthin in liver: potential role of cytokine-mediated cell-cell interactions. Food Funct 11:9252–9262. https://doi.org/10.1039/d0fo01223h

80. Zhao JY, Bi W, Zhang JW, Xiao S, Zhou RY, Tsang CK, Lu DX, Zhu L (2020) USP8 protects against lipopolysaccharide-induced cognitive and motor deficits by modulating microglia phenotypes through TLR4/MyD88/NF-κB signaling pathway in mice. Brain Behav Immun 88:582–596. https://doi.org/10.1016/j.bbi.2020.04.052

81. Liu BY, Yu HX, Baiyun RQ, Lu JJ, Li SY, Bing QZ, Zhang XY, Zhang ZG (2018) Protective effects of dietary luteolin against mercuric chloride-induced lung injury in mice: involvement of AKT/Nrf2 and NF-κB pathways. Food Chem Toxicol 113:296–302. https://doi.org/10.1016/j.fct.2018.02.003

82. Tedgui A, Mallat Z (2006) Cytokines in atherosclerosis: pathogenic and regulatory pathways. Physiol Rev 86:515–581. https://doi.org/10.1152/physrev.00024.2005

83. Zhu XJ, Yao YY, Yang JR, Zhengxie JH, Li XY, Hu SJ, Zhang A, Dong JD, Zhang CC, Gan GM (2020) COX-2-PGE2 signaling pathway contributes to hippocampal neuronal injury and cognitive impairment in PTZ-kindled epilepsy mice. Int Immunopharmacol 87:106801. https://doi.org/10.1016/j.intimp.2020.106801

84. Wei ZJ, Nie GH, Yang F, Pi SX, Wang C, Cao HB, Guo XQ, Liu P, Li GY, Hu GL, Zhang CY (2020) Inhibition of ROS/NLRP3/Caspase-1 mediated pyroptosis attenuates cadmium-induced apoptosis in duck renal tubular epithelial cells. Environ Pollut 273:115919. https://doi.org/10.1016/j.envpol.2020.115919

85. Zhang F, Yu W, Hargrove JL, Greenspan P, Dean RG, Taylor EW, Hartle DK (2002) Inhibition of TNF-alpha induced ICAM-1, VCAM-1 and E-selectin expression by selenium. Atherosclerosis 161:381–386. https://doi.org/10.1016/s0021-9150(01)00672-4

86. Kim SH, Johnson VJ, Shin TY, Sharma RP (2004) Selenium attenuates lipopolysaccharide-induced oxidative stress responses through modulation of p38 MAPK and NF-kappaB signaling pathways. Exp Biol Med (Maywood) 229:203–213. https://doi.org/10.1177/153537020422900209

87. Zamamiri-Davis F, Lu Y, Thompson JT, Prabhu KS, Reddy PV, Sordillo LM, Reddy CC (2002) Nuclear factor-kappaB mediates over-expression of cyclooxygenase-2 during activation of RAW 264.7 macrophages in selenium deficiency. Free Radic Biol Med 32:890–897. https://doi.org/10.1016/s0891-5849(02)00775-x

88. Yang DQ, Tan X, Lv ZJ, Liu BY, Baiyun RQ, Lu JJ, Zhang ZG (2016) Regulation of Sirt1/Nrf2/TNF-α signaling pathway by luteolin is critical to attenuate acute mercuric chloride exposure induced hepatotoxicity. Sci Rep 6:37157. https://doi.org/10.1038/srep37157

89. Liu ZW, Wang JK, Qiu C, Guan GC, Liu XH, Li SJ, Deng ZR (2015) Matrine pretreatment improves cardiac function in rats with diabetic cardiomyopathy via suppressing ROS/TLR-4 signaling pathway. Acta Pharmacol Sin 36:323–333. https://doi.org/10.1038/aps.2014.127

90. Liu ZW, Zhu HT, Chen KL, Qiu C, Tang KF, Niu XL (2013) Selenium attenuates high glucose-induced ROS/TLR-4 involved apoptosis of rat cardiomyocyte. Biol Trace Elem Res 156:262–270. https://doi.org/10.1007/s12011-013-9857-7

91. Zhong XM, Zhang L, Li YM, Li P, Li J, Cheng GC (2018) Kaempferol alleviates ox-LDL-induced apoptosis by up-regulation of miR-26a-5p via inhibiting TLR4/NF-κB pathway in human endothelial cells. Biomed Pharmacother 108:1783–1789. https://doi.org/10.1016/j.biopha.2018.09.175

92. Huang DJ, Li Y, Yang ZX, Sun YN, Wan D (2019) Association of the TLR4-MyD88-JNK signaling pathway with inflammatory response in intracranial hemorrhage rats and its effect on neuronal apoptosis. Eur Rev Med Pharmacol Sci 23:4882–4889. https://doi.org/10.26355/eurrev_201906_18076

93. Wang L, Song LF, Chen XY, Ma YL, Suo JF, Shi JH, Chen GH (2019) MiR-181b inhibits P38/JNK signaling pathway to attenuate autophagy and apoptosis in juvenile rats with kainic acid-induced epilepsy via targeting TLR4. CNS Neurosci Ther 25:112–122. https://doi.org/10.1111/cns.12991

94. Yang DQ, Han B, Baiyun RQ, Lv ZJ, Wang XQ, Li SY, Lv YY, Xue JD, Liu Y, Zhang ZG (2020) Sulforaphane attenuates hexavalent chromium-induced cardiotoxicity via the activation of the Sesn2/AMPK/Nrf2 signaling pathway. Metallomics 12:2009–2020. https://doi.org/10.1039/d0mt00124d

95. Yang DQ, Yang QY, Fu N, Li SY, Han B, Liu Y, Baiyun RQ, Lu JJ, Zhang ZG (2021) Hexavalent chromium induced heart dysfunction via Sesn2-mediated impairment of mitochondrial function and energy supply. Chemosphere 264:128547. https://doi.org/10.1016/j.chemosphere.2020.128547

96. Yang QY, Han B, Xue JD, Lv YY, Li SY, Liu Y, Wu PF, Wang XQ, Zhang ZG (2020) Hexavalent chromium induces mitochondrial dynamics disorder in rat liver by inhibiting AMPK/PGC-1α signaling pathway. Environ Pollut 265:114855. https://doi.org/10.1016/j.envpol.2020.114855